OFFPRINTS FROM: MONSOONS
Edited by Dr. Jay S. Fein and Dr. Pamela L. Stephens

16

Long-Range Forecasting of Monsoons

J. Shukla
Center for Ocean–Land–Atmosphere Interactions
Department of Meteorology
University of Maryland
College Park, Maryland

INTRODUCTION

As discussed in Chapter 14, the day-to-day changes in weather are mainly due to the growth, propagation, and decay of the synoptic-scale disturbances that owe their origin to the instabilities of the large-scale flow. The growth rate for the dominant instabilities and their nonlinear interactions with other scales and the mean flow are such that these synoptic-scale disturbances become totally unpredictable within a couple of weeks. This limit of deterministic predictability has been the greatest stumbling block for progress in dynamical, long-range forecasting, and therefore, it is no surprise that in the past most of the attempts at long-range forecasting have been either synoptic or statistical in nature.

Recent observational and modeling studies have suggested that although the synoptic scales lose their predictability within two weeks, the low-frequency planetary scales remain predictable up to a month (1). It has also been suggested that there may be additional predictability due to the influence of the slowly varying boundary conditions at the earth's surface (2). The situation is especially promising in the low latitudes where synoptic scale instabilities are too weak to degrade the predictability of the large scales, and the influence of the changes in the boundary conditions is large enough to be clearly distinguishable from the unpredictable day-to-day fluctuations. These results, collectively, have suggested a physical basisfor dynamical prediction of average monthly and seasonal atmospheric conditions.

Section 1 describes the current status of our knowledge of the long-range predictability of monsoons. Section 2 covers the operational statistical forecasting of seasonal monsoon rainfall over India and Section 3 presents a new and simple technique for predicting summer monsoon rainfall over India.

1 PREDICTABILITY OF MONSOONS

Charney and Shukla (3) have suggested that low-latitude atmospheric flows in general, and the monsoon circulations in particular, are potentially more predictable than mid-latitude circulations. This suggestion was based on the results of observational, theoretical, and numerical studies which show that: the day-to-day fluctuations in the tropics are small, implying weak flow instabilities; the interannual fluctuations of seasonal averages are large and are related to the changes in the boundary conditions of such slowly varying parameters as sea surface temperature, soil moisture, albedo, and vegetation; and numerical simulations by general circulation models with prescribed boundary conditions underestimate the observed low-latitude variability. The planetary-scale tropical circulations are dominated by thermally forced Hadley and Walker type circulations (see Chapter 11), which are intrinsically stable because weak tropical disturbances cannot change them, and also because they are linked with slowly varying boundary conditions. Since the space and time averages in the tropics are dominated by the large-scale, low-frequency components, monthly and seasonal predictions are possible, even if the weak, synoptic-scale instabilities are not predictable on the shorter time scales.

Charney and Shukla (3) examined the variability among four July simulations with a global general circulation model (4) in which the global boundary conditions were identical but the initial conditions different. The observed initial conditions in the middle of June were altered at all the model grid points by superimposing random error fields of wind, temperature, and pressure. The spatial structure of the random error fields corresponded to Gaussian distributions with zero means and standard deviations of 1°C in temperature, 3 m/sec in horizontal wind components and 1 mb in surface pressure. The initial perturbation fields were quite large, at least for the tropics. The simulated fields were quite different at the end of 15 model days of integration. The first two weeks of integrations were ignored and monthly averages for July (days 16–46) sea level pressure and rainfall were calculated for each of the four simulations. Figure 16.1 shows the model (σ_M) and observed (σ_O) zonally averaged standard deviations and their ratios for July sea level pressure and rainfall as functions of latitude. The observed standard deviations were calculated for about 380 Northern Hemisphere stations for 10 years (1966–1975). It can be seen that the observed and the model simulated variabilities are comparable in mid-latitudes, but the variability in the simulations is considerably less than that observed in the low latitudes. The ratios of the observed and the model standard deviations are less than 1.5 between the latitudes 25°N and 55°N for pressure and to the north of 30°N for rainfall. For low latitudes, the ratio is more than 2.0. Similar results were obtained for the averages over limited areas in low and middle latitudes.

Manabe and Hahn (5) have carried out an 18-year integration of the GFDL (Geophysical Fluid Dynamics Laboratory) spectral model with prescribed seasonally varying but interannually fixed boundary conditions of sea surface temperature. Figure 16.2 shows the zonally averaged standard deviation of winter season 1000-mb geopotential height for the last 15 years of their simulation (σ_M), the observations (σ_O), the ratio (σ_O/σ_M). The ratio of observed and simulated standard deviations

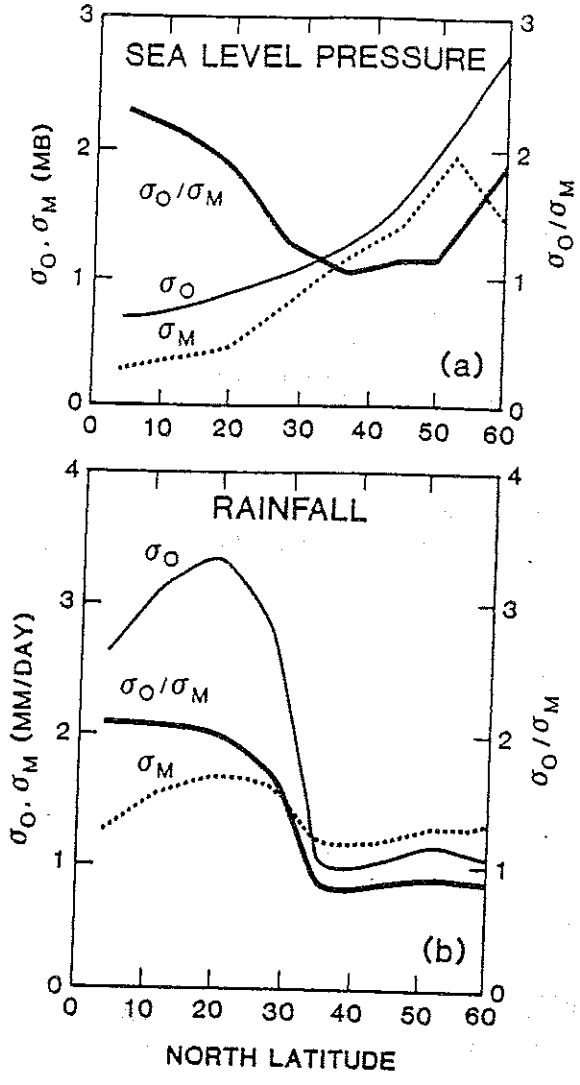

Figure 16.1. Model (σ_M, dotted line) and observed (σ_O, thin solid line) zonally averaged standard deviations as functions of latitude, and their ratio (σ_O/σ_M, thick solid line), for mean July: (*a*) sea level pressure and (*b*) rainfall. Observed values are for land stations and model values are for grid points over land. Reprinted with permission from the Cambridge University Press from Charney and Shukla, *Monsoon Dynamics* (reference 3).

is about 2.0 in the near-equatorial regions and about 1.0 in the middle and high latitudes. This ratio was found to be more than 3.0 for tropical upper tropospheric variables. If we can assume that this discrepancy in observed and simulated variability at low latitudes was not due to model deficiencies, Manabe and Hahn's results from a completely different model and based on long-term simulations provide further evidence for Charney and Shukla's (3) results.

Based on these results, Charney and Shukla proposed that the cause of the discrepancy between model and observed variability in the low latitudes could be the boundary conditions that were fixed and constant for all the simulations. This hypothesis is supported by observed correlations between boundary conditions and circulation patterns, and sensitivity experiments with global models which show that tropical boundary anomalies produce significant changes in the model simulated circulation and rainfall. There is a serious limitation to studies that compare model and observed variability because model deficiencies can also produce an underestimate of the interannual variability. Although in the Charney and Shukla study the day-to-day model fluctuations were quite realistic when compared to the observations, it would have been more appropriate to compare the variabilities of

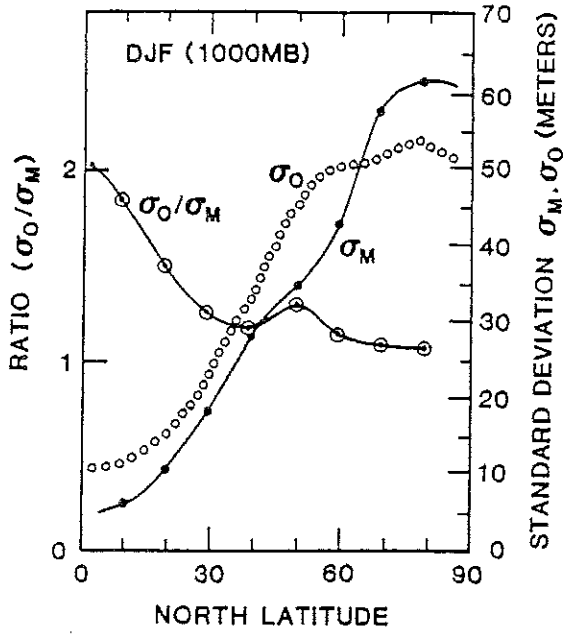

Figure 16.2. Zonally averaged means of standard deviation of seasonal mean 1000-mb geopotential height in meters; observations (σ_O, broken line of circles) and model (σ_M, solid line with black dots). On the left side is the ratio (σ_O/σ_M, solid line with circles) of observed and model standard deviations. Reprinted with permission from the American Meteorological Society from Manabe and Hahn, *Monthly Weather Review* (reference 5).

same model with and without changes in the boundary conditions. The following results describe such an experiment which was carried out with the GLAS (Goddard Laboratory for Atmospheric Sciences) general circulation model (6).

A 45-day integration was carried out starting from observed initial conditions in the middle of June, and long-term climatological mean boundary conditions of sea surface temperature (SST). This integration is referred to as the control run (C). For the identical boundary conditions, three additional integrations of 45 days each were carried out by randomly changing the initial conditions of the horizontal wind components u and v at each of the nine levels of the model. The spatial structure of the random errors corresponded to a Gaussian distribution with zero mean and standard deviation of 3 m/sec for each of u and v. These three integrations are referred to as predictability runs (P_1, P_2, and P_3). Although the statistical properties of the random errors were the same for each predictability run, the actual grid point values were randomly different. Three additional integrations were carried out for which, in addition to the randomly perturbed initial conditions, the climatological boundary conditions of SST between the equator and 30°N were replaced by each year's observed monthly mean SST during July of 1972, 1973, and 1974. These three integrations are referred to as boundary forcing runs (B_1, B_2, and B_3).

The variance $(\sigma_P)^2$ among C, P_1, P_2, and P_3 is a measure of the natural variability of the model; the variance $(\sigma_B)^2$ among C, B_1, B_2, and B_3 is a measure of the variability due to changes in the boundary conditions of the tropical SST.

$$(\sigma_P)^2_{i,j} = 1/3\ [(C - \overline{P})^2 + (P_1 - \overline{P})^2 + (P_2 - \overline{P})^2 + (P_3 - \overline{P})^2]_{i,j} \quad (1)$$

$$(\sigma_B)^2_{i,j} = 1/3\ [(C - \overline{B})^2 + (B_1 - \overline{B})^2 + (B_2 - \overline{B})^2 + (B_3 - \overline{B})^2]_{i,j} \quad (2)$$

where $\overline{P} = (C + P_1 + P_2 + P_3)/4$ and $\overline{B} = (C + B_1 + B_2 + B_3)/4$, and C_{ij}, P_{ij}, B_{ij} denote the July mean at grid point i,j.

Figure 16.3 shows the plots of zonally averaged values of standard deviations σ_P, σ_B, σ_O and the ratios σ_O/σ_P and σ_O/σ_B where σ_O is the standard deviation for 10 years of observed monthly means. In agreement with the results of Charney and Shukla (3), it is seen that the ratio σ_O/σ_P is more than 2.0 in the tropical latitudes and close to 1.0 in the middle latitudes. The new result is that the curve σ_B lies nearly halfway between the curves σ_O and σ_P. This suggests that for this model about half of the "unexplained" variability is accounted for by changes in sea surface temperature between the equator and 30°N.

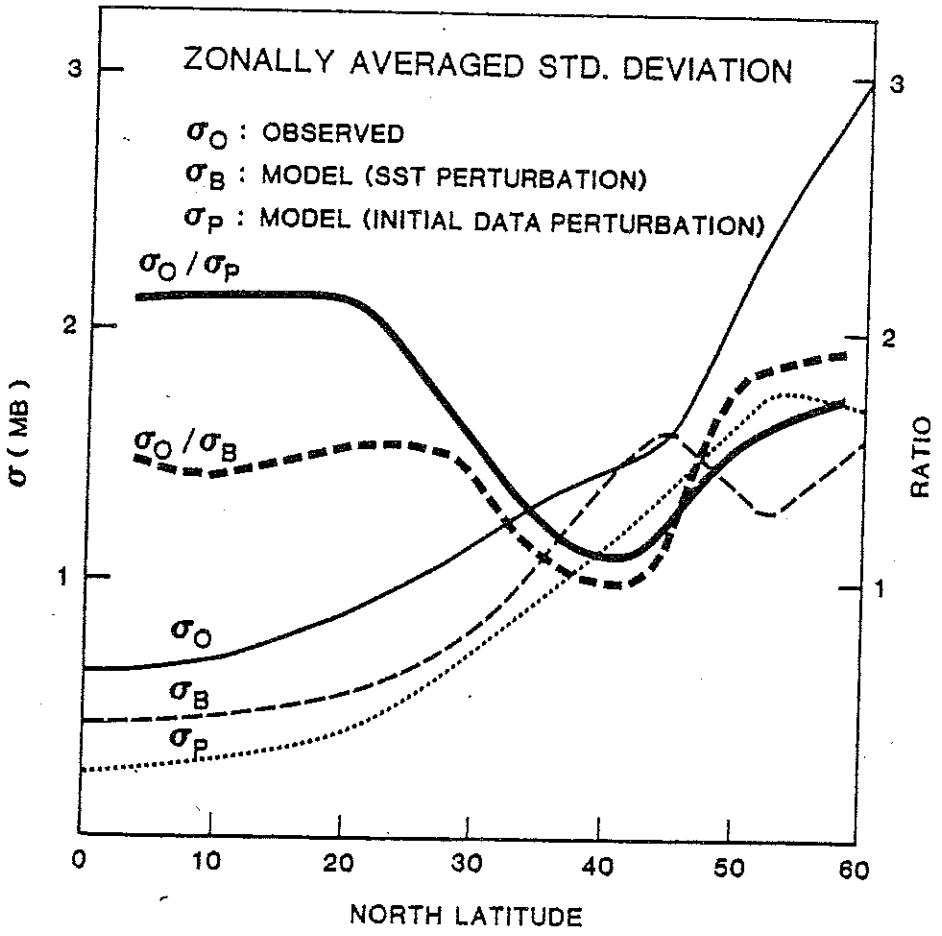

Figure 16.3. Zonally averaged standard deviation of monthly mean (July) sea level pressure (mb) for 10 years of observations (σ_O, thin solid line), four model runs with variable boundary and initial conditions (σ_B, thin dashed line), and four model runs with identical boundary conditions (σ_P, thin dotted line). Thick solid line and thick dashed line show the ratio σ_O/σ_P and σ_O/σ_B, respectively (from reference 6)

This supports Charney and Shukla's hypothesis that the slowly varying boundary conditions play an important role in determining the interannual variability of time averages for the tropical atmosphere. Additional effects of soil moisture or the Eurasian snow cover could possibly bring the σ_O and σ_B curves still closer. However, since the long period internal dynamical changes (e.g., tropical–extratropical interactions) can also contribute to the interannual variability of time averages, it would never be possible to explain the total σ_O by boundary conditions alone.

The model variability for the predictability and boundary forcing integrations have also been compared. Since the SST anomalies for B_1, B_2, and B_3 have many common features, it is more appropriate to calculate the changes in the monthly means due to boundary conditions (E_B) and due to random perturbations (E_P) as follows:

$$E_B^2 = 1/3 \sum_{k=1}^{3} (C - B_k)^2 \qquad \text{(at each grid point } i,j) \tag{3}$$

and

$$E_P^2 = 1/3 \sum_{k=1}^{3} (C - P_k)^2 \qquad \text{(at each grid point } i,j) \tag{4}$$

Figure 16.4 shows the zonally averaged values of E_B and E_P for July mean geopotential height at 300 mb. In agreement with the observations in the atmosphere the values of E_B and E_P are small for the low latitudes and large for the middle latitudes. However, in this experiment, the ratio E_B/E_P is more than 2.0 for low latitudes. The largest values of the ratio E_B/E_P occur between 20°N–20°S. This result also suggests a possible role of tropical SST anomalies for changes in the atmospheric circulation away from the SST anomalies. Although the SST boundary anomalies were imposed only between the latitudes 0–30°N, their effects on the circulation at 300 mb are seen in the Southern Hemisphere tropics also. This could be either due to meridionally propagating Rossby waves forced by heating due to the SST anomalies, or interhemispheric interactions associated with the fluctuations of Hadley cells which are strongly influenced by SST anomalies and their attendant convection (see Chapter 11). The results for geopotential height at 500 mb (not shown) are very similar to those shown in Figure 16.4 except that the peak of the ratio E_B/E_P at the equator is not as high.

Lau (7) has further analyzed the model simulations of Manabe and Hahn (who, we will recall, used interannually fixed boundary conditions of SST), and found that the model simulated mass field did not show any evidence of the Southern Oscillation, which is clearly seen in the observations as pressure anomalies of opposite sign in the Indian Ocean and the eastern equatorial Pacific. This gives indirect evidence for the importance of tropical SST anomalies for the Southern Oscillation.

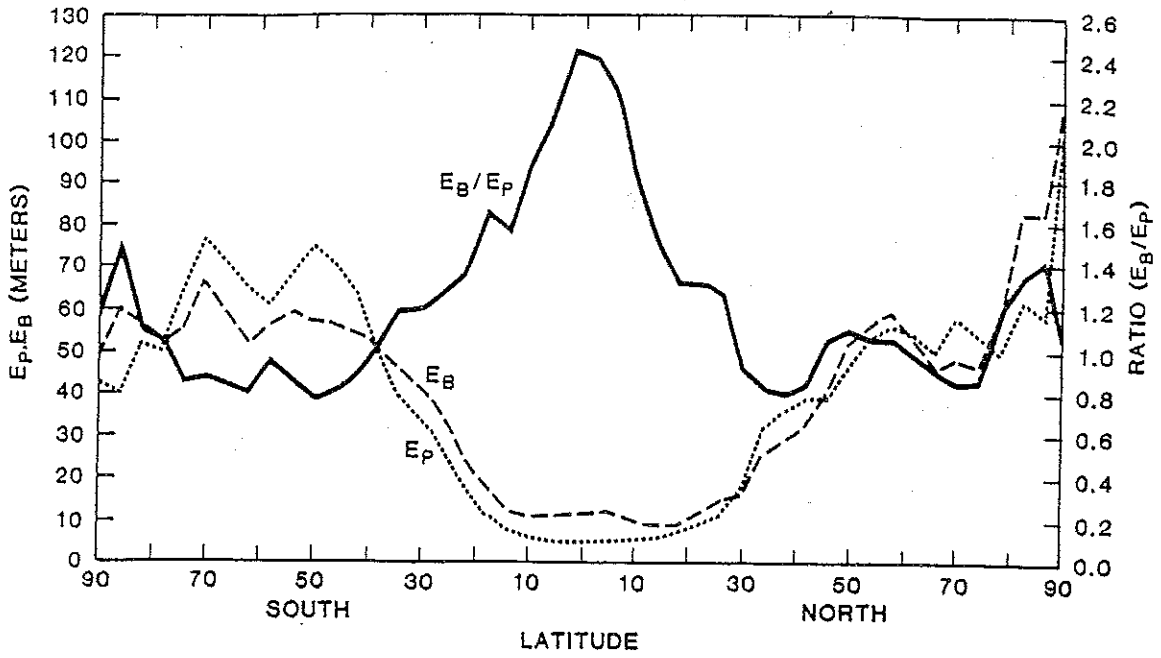

Figure 16.4. Zonally averaged standard deviation for predictability runs (E_P, dotted line), boundary forced runs (E_B, dashed line) and the ratio of boundary forced and predictability runs (E_B/E_P, thick solid line) for geopotential height at 300 mb (from reference 6).

The numerical results of Charney and Shukla (3), Shukla (6), Manabe and Hahn (5), and Lau (7) provide strong, albeit indirect, evidence that SST anomalies in the tropics are one of the most important determinants of the interannual variability of the tropical and monsoonal circulations. These results are also in agreement with Madden (8) who examined the predictability of monthly sea level pressure over the Northern Hemisphere. He compared the variances of the observed monthly means with the "natural variability" of monthly means that occur in the absence of boundary forcing and showed that the long period changes in low latitudes are potentially more predictable compared to those in the mid-latitudes. These conclusions are further confirmed by the results of Shukla and Gutzler (9).

In addition to the above mentioned "indirect" numerical and observational results, there is a large body of literature on numerical experiments with global general circulation models which show, more directly, the sensitivity of model climate to changes in the boundary conditions. The following brief description is presented of the physical mechanisms through which properly specified boundary conditions can enhance the predictability of monthly and seasonal atmospheric averages.

1.1 Boundary Forced Predictability

Simple arguments suggest that enhanced atmospheric predictability on monthly and seasonal time scales is possible with the proper specifications of boundary effects. The mechanisms involved are different for each boundary type.

1. Changes in boundary forcing directly influences the location and intensity of the heat sources and sinks that drive the atmospheric circulation. The forcing at the boundary itself is generally not sufficient to produce significant changes in the atmospheric circulation; however, under favorable conditions of large-scale convergence and divergence, the boundary effect is transmitted through the atmosphere, transforming a shallow boundary forcing into a three-dimensional change in heating distributions which can be quite effective in influencing the atmospheric circulation. The effectiveness of a boundary forcing in changing the atmospheric circulation therefore strongly depends upon its ability to produce a deep heat source and a means by which this influence can propagate away from the source. Since both of these factors are determined by the structure of the large-scale dynamical circulation itself, the response of a given boundary forcing can be very different depending upon its size and geographical location, and on the structure of the large-scale circulation.

2. Boundary forcings of SST, soil moisture, surface albedo, and snow and ice not only affect the sources and sinks of heat, but they also affect the sources and sinks of moisture, and in turn, the latent heat sources.

3. The strongly nonlinear character of the atmosphere is such that even a weak anomaly in a boundary forcing, under favorable conditions, can produce significant anomalies in atmospheric circulation, and therefore the actual response may be stronger than one estimated from linear theories.

1.1.1 Snow Cover. Large-scale anomalies of snow cover have the potential to influence the atmospheric circulation by several physical processes:

1. An increase in snow cover increases the albedo, and therefore reduces the incoming solar radiation. If there were no other feedbacks, this would produce colder temperatures (and also result in the snow cover anomalies persisting for a longer time).

2. Excessive snow anomalies in the mid-latitudes, by cooling the overlying air, can act as anomalous heat sinks which in turn can produce anomalous stationary wave patterns that can alter storm tracks and their frequency.

3. Persistent snow anomalies can change the components of the heat balance of the earth's surface. Even after the snow has melted completely, wet soil will maintain colder surface temperatures for longer periods of time than dry soil.

4. Persistent snow anomalies can produce anomalous meridional temperature gradients and associated anomalous vertical wind shears which in turn can change the instability characteristics of synoptic-scale weather disturbances.

1.1.2 Sea Surface Temperature. The factors that determine the influence of SST anomalies on the atmospheric circulation are rather complex. The immediate effect of an SST anomaly is to change the sensible heat flux and evaporation in its immediate vicinity. However, this type of thermal forcing, confined to the ocean's surface, is too weak to produce significant changes in the atmospheric circulation. The crucial factor that determines whether an SST anomaly can affect the atmospheric

the heat sources over these areas could produce considerable change in the planetary-scale circulations of the tropical as well as the extratropical atmosphere. Despite the small (relative to the oceans) earth surface area covered by land, the soil moisture effects over land could be as important as SST anomaly effects. The soil moisture effects depend strongly upon season and latitude. During the winter season in high latitudes, the amount of solar radiation reaching the ground is not large enough to significantly alter the surface energy budget. Changes in soil moisture influence evaporation and heating of the land surface. The degree to which the total radiative energy impinging on the ground goes into latent rather than sensible heating is determined by the wetness of the ground. If the soil is wet, most of the radiative energy goes to evaporate the water, if the soil is dry and there is no vegetation, most of the radiative energy is used to heat the ground and the overlying air.

This discussion of the mechanisms through which boundary forcing influences the atmospheric circulation suggests that there is a physical basis for prediction of monthly and seasonal atmospheric anomalies due to the influence of boundary conditions. Since the boundary conditions change slowly, they can be prescribed and their effects on the atmosphere can be calculated using a dynamical model. Recognition of the importance of the boundary conditions for extended range predictability is an important step toward dynamical long-range forecasting that can now be attempted using current models and global observations of the boundary conditions.

2 FORECASTING OF SEASONAL RAINFALL OVER INDIA

After India experienced a great famine in 1877, a year with highly deficient summer monsoon rainfall over most of the country, the British Government called upon Henry F. Blanford to make monsoon forecasts. Blanford was a geologist and the first Meteorological Reporter for Bengal. He established the India Meteorological Department in 1875 and served as its director. Blanford (11) noted an association between large winter and spring snowfalls in the Himalayas and monsoon droughts over India in summer and he used this association to make preliminary forecasts during 1882–1885. He met with some success and official forecasts were issued beginning in 1886. Sir John Eliot, who succeeded Blanford, used weather conditions over the whole of India and the surrounding regions to prepare elaborate (perhaps too elaborate—as long as 30 pages) forecasts of monsoon rainfall. India experienced another great famine in 1899 and the newspapers were so critical of the long-range forecasts of the monsoon rainfall that for some time the forecasts were issued only to the Provincial Governments as confidential documents. Sir Gilbert T. Walker, a Senior Wrangler at Cambridge, succeeded Eliot and started objective methods of monsoon rainfall forecasting based on correlation. While searching for the potential predictors of Indian monsoon rainfall, and benefiting from the earlier work of Eliot, who had noted an association between high pressure over Mauritius and Australia, and droughts over India, Walker described and coined the words the "Southern Oscillation," as well as the two "Northern Oscillations" (North Atlantic and North

Pacific). Walker's search for global predictors at large distances away from India was motivated by the already published papers of Hildebrandsson (12) who had noted an opposite polarity of pressure at Sydney and Buenos Aires, and the Lockyers (13) who had further confirmed the pressure seesaw between the Indian Ocean and Argentina (14). In Chapter 8, G. Kutzbach provides a detailed description of this productive period in India's history.

Walker (15) developed several regression formulas to predict seasonal monsoon rainfall averaged over homogeneous subdivisions of India. A comprehensive review of the method, the factors used as predictors, and the performance of these methods has been documented by Jagannathan (16). The regression formulas used by Walker in 1924 for forecasting seasonal (June–September) rainfall over Peninsula and Northwest India (which are defined in Chapter 14, Fig. 14.5) are given below as an example:

Peninsula rainfall departure in inches

$$= 1.61\,F_1 - 0.29\,F_2 - 0.02\,F_3 - 77.3\,F_4 - 0.21\,F_5 - 0.35\,F_6 \quad (5)$$

Northwest rainfall departure in inches

$$= 0.29\,F_1 - 44.5\,F_4 - 0.36\,F_5 - 0.95\,F_7 - 0.53\,F_8 - 17.0\,F_9 \quad (6)$$

where F_1 = average of April and May departure from normal pressure averaged for Santiago, Buenos Aires, and Cordoba (mm of mercury),

F_2 = May Zanzibar percentage rainfall departure from normal,

F_3 = October through February Java percentage rainfall departure from normal,

F_4 = average of September, October, and November Capetown pressure departure (inches of mercury),

F_5 = October through April South Rhodesian rainfall departure from normal (inches),

F_6 = average of March and April Dutch Harbor temperature (degrees F),

F_7 = snow accumulation in Himalayas by end of May (tabulated on a numerical scale of departure),

F_8 = average of December through April Dutch Harbor temperature (degrees F), and

F_9 = average of: average February and March Seychelles pressure, average January through April Batavia pressure, and average March through May Port Darwin pressure departures (inches of mercury).

These regression equations were revised periodically to include new predictors and modified values of regression coefficients for old predictors. The following regression equation was used by the India Meteorological Department to predict Peninsula rainfall for the summer monsoon season of 1954 (17).

Peninsula rainfall departure in inches

$$= 1.825\,X_1 + 0.912\,X_2 - 0.067\,X_3 - 0.0183\,X_4 - 0.559\,X_5 + 4.287$$

where X_1 = average of April and May departure from normal pressure for Santiago, Buenos Aires, and Cordoba (in mm of mercury),
X_2 = average April northerly wind speed (m/sec) over Bangalore at 6 km,
X_3 = October through April South Rhodesia rainfall departure from normal (in inches),
X_4 = October through February Java percentage rainfall departure from normal, and
X_5 = average May easterly wind speed (m/sec) over Calcutta at 4 km.

Eq. (7) shows that by the mid-1950s, upper air predictors had been included in the forecast schemes. The equations currently in use in India have been modified still further. They are discussed by Das (see Section 3.2.1 of Chapter 17).

From a close examination of the various predictors used during the past 60 years, with the possible exception of the Southern Oscillation and related circulation features, a physical basis for these statistical relationships is not clear. It is likely that these apparent relationships are due simply to random sampling; however, a definitive conclusion cannot be drawn without a detailed examination of the long-term variability of these predictors. A superficial analysis of available data suggests that most of the predictors chosen by Walker are indirect descriptors of the Southern Oscillation phenomenon.

Normand (14) verified 18 years (1931–1948) of forecasts of monsoon rainfall. Thirty-two cases were for the summer season of June through September (16 for Northwest and 16 for Peninsula India), 29 were for only August and September (15 for Northwest and 14 for Peninsula India), and nine cases were for the Northwest for the winter season of January through March. He showed that forecasts were considerably better than those based on pure chance, but only slightly better than those based on probability tables for odds of 4 to 1 against being wrong. Verification for the deficient rainfall years alone showed that 66% of these forecasts were wrong. For August and September rainfall over Northwest India, forecasts for all the seven years of deficient rainfall were wrong. Normand wondered whether these forecasts were of any use at all; however, he favored continuation, "if only to keep the subject alive and in the hope that ideas for progress will emerge." Unfortunately there is no available documentation for the performance of the regression equations for the last 20 years.

3 THE RELATIONSHIP BETWEEN THE SOUTHERN OSCILLATION AND MONSOON RAINFALL

As discussed in the preceding section, relationships between the Southern Oscillation and the Indian monsoon rainfall were established by Walker in the beginning of this century and versions of them have been used since for operational forecasting of monsoon rainfall. This section re-examines the relationship between the Southern Oscillation and Indian monsoon rainfall using the Darwin sea level pressures for the period 1901–1981, and the summer monsoon rainfall data described in Chapter 14. Darwin pressure was chosen because its long term record is considered to be

more accurate and more complete than that for any other station in that region. Although Tahiti minus Darwin pressure is considered to be a better index of the Southern Oscillation, Tahiti pressure is available only for the period 1935–1981, and for this period the correlation coefficient between the spring Tahiti pressure and Indian monsoon rainfall is only 0.01. The summer monsoon rainfall data used in this study is the area weighted average of the percentage departures for each of the 31 subdivisions of India, and is referred to as the whole Indian monsoon rainfall anomaly in Chapter 14.

3.1 Influence of the Southern Oscillation on Summer Monsoon Rainfall over India

Figure 16.5 shows the data used: the thin line denotes the 12-month running mean of the normalized Darwin pressure anomaly and the bars denote the normalized Indian monsoon rainfall anomaly. For normalization, the anomaly is divided by its

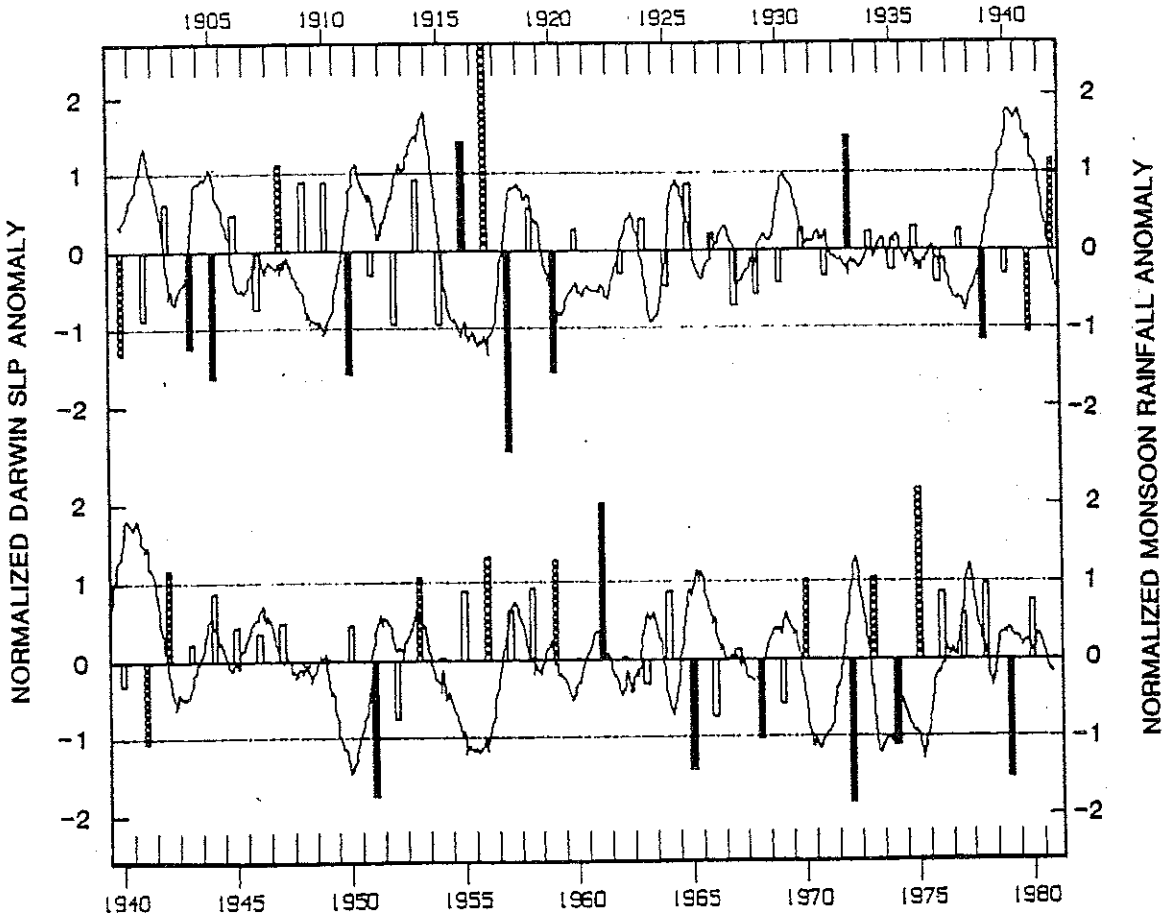

Figure 16.5. Twelve-month running mean of normalized monthly Darwin pressure anomaly (thin line) and normalized Indian monsoon rainfall anomaly (bars). Years with normalized rainfall anomaly of more than 1.0 or less than −1.0 standard deviation are shown by solid black bars for positive, and hatched bars for negative trend of the Darwin pressure anomaly. Reprinted with permission from the American Meteorological Society from Shukla and Paolino, *Monthly Weather Review*, **111**, 1830–1837 (1983).

standard deviation. The normalized rainfall anomaly is more than one standard deviation for the years 1908, 1916, 1917, 1933, 1942, 1953, 1956, 1959, 1961, 1970, 1973, and 1975, and is less than minus one standard deviation for the years 1901, 1904, 1905, 1911, 1918, 1920, 1939, 1941, 1951, 1965, 1968, 1972, 1974, and 1979. The former group of years will be referred to as the heavy monsoon rainfall years and the latter as the deficient monsoon rainfall years. The composite normalized seasonal mean Darwin pressure anomalies averaged for all the heavy rainfall years, and the deficient rainfall years, are shown in Figure 16.6. The rectangle on the graph denotes the summer season for which the monsoon rainfall was considered, and the following and the preceding months are represented along the abscissa to the right and to the left. Along the ordinate are the values of the composite, 3-month running mean, pressure anomaly.

The most remarkable feature of this figure is the simultaneous occurrence of high (low) Darwin pressure anomalies and deficient (heavy) monsoon rainfall anomalies that persist for two seasons after the monsoon. This association, however, has little usefulness for the long-range forecasting of the monsoon rainfall. For the purpose of predicting the monsoon rainfall, the most useful antecedent parameter appears to be the *trend* of the Darwin pressure anomaly before the monsoon season. The Darwin pressure anomaly decreases from winter to spring before the heavy rainfall years, and increases before the deficient rainfall years. The value of the

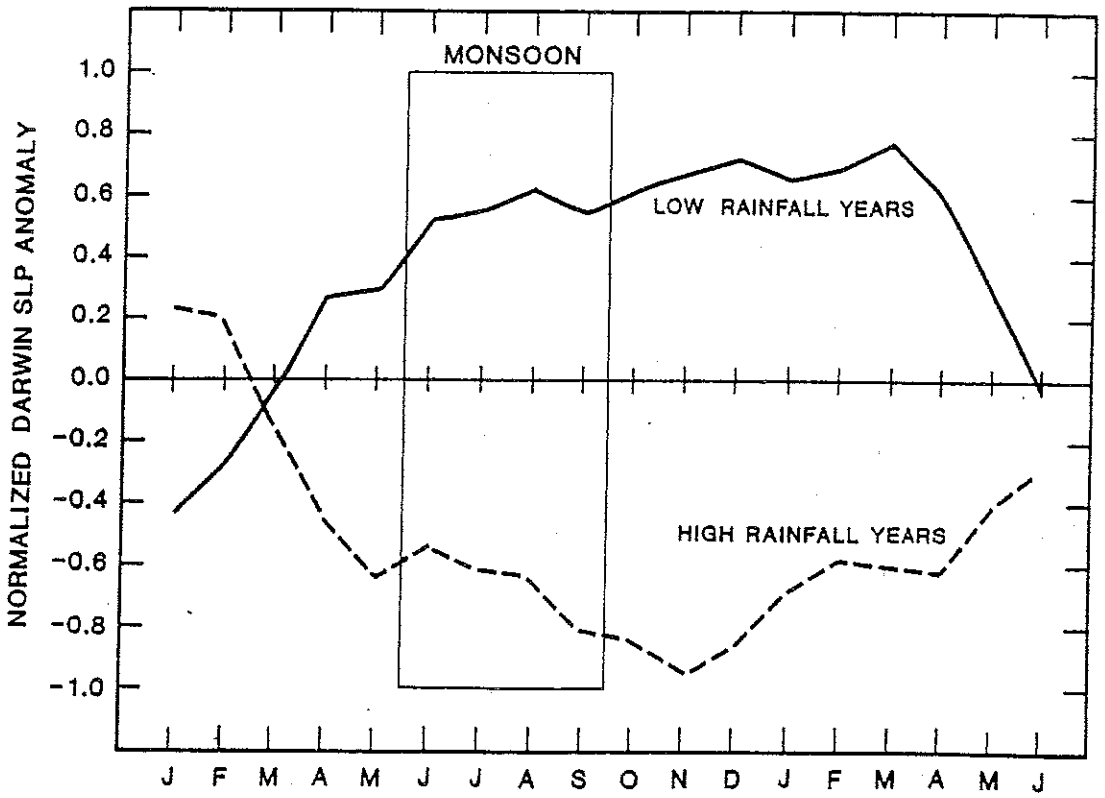

Figure 16.6. Composite of normalized Darwin pressure anomaly (3-month running mean) for heavy monsoon (high) rainfall years and deficient monsoon (low) rainfall years. Reprinted with permission from the American Meteorological Society from Shukla and Paolino, *Monthly Weather Review*, **111**, 1830–1837 (1983).

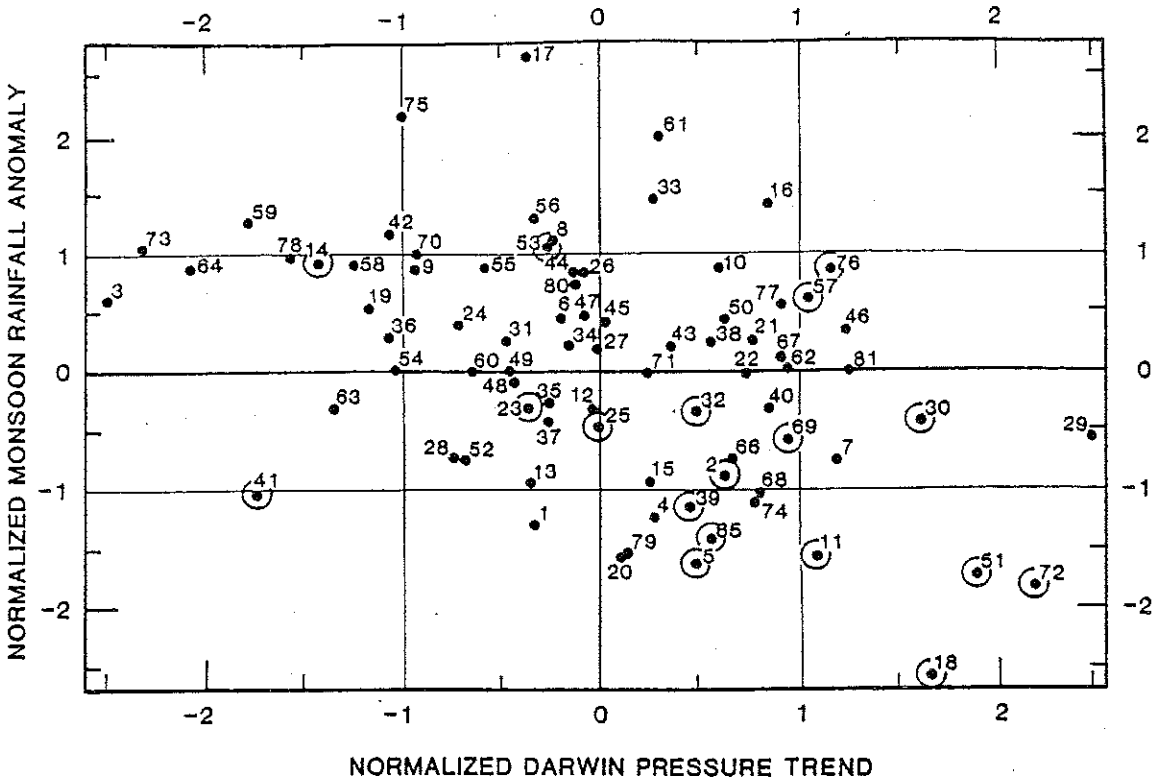

Figure 16.7. Scatter diagram between the normalized Darwin pressure trend (spring–winter) along the abscissa, and normalized Indian monsoon rainfall anomaly along the ordinate. The numbers denote the year (minus 1900). Open circles represent El Niño years. Reprinted with permission from the American Meteorological Society from Shukla and Paolino, *Monthly Weather Review*, **111**, 1830–1837 (1983).

Darwin pressure anomaly itself during the preceding winter and spring does not appear to be a useful parameter because it fluctuates around zero. We have therefore examined the association between the Darwin pressure trend and summer monsoon rainfall over India. The Darwin pressure trend is defined as the spring (March, April, May) minus the winter (December, January, February) pressure anomaly. The correlation coefficient between the normalized monsoon rainfall anomaly and the difference of the normalized spring and winter Darwin pressure anomaly is -0.46, which, in absolute value, is higher than that for the normalized spring Darwin pressure anomaly (0.32). The correlation coefficient between the normalized Darwin pressure trend and the Indian rainfall anomaly is -0.42. I am not aware of any other antecedent parameter with a correlation coefficient with the monsoon rainfall as high as -0.42 for a time series as long as 81 years. Pant and Parthasarthy (18) have shown that the correlation coefficient between a Southern Oscillation index [as defined by Wright (19) which consists of surface pressure averaged for several stations] and monsoon rainfall is 0.34.

Figure 16.7 shows a scatter diagram between the normalized Darwin pressure trend and the normalized Indian monsoon rainfall anomaly. Most of the severe drought years are in the lower right quadrant, and most of the excessive rainfall years are in the upper left quadrant of the scatter diagram. During the 81-year

period examined here, there were only two occasions (1901 and 1941) when a negative Darwin pressure trend was followed by a negative normalized rainfall anomaly greater than −1.0. The near absence of points in the lower left corner of this scatter diagram suggests that a negative Darwin pressure trend is a very useful predictor for the nonoccurrence of droughts over India. Similarly a positive Darwin pressure trend can be a good predictor for the nonoccurrence of excessive rain.

Rasmusson and Carpenter (20) have identified 18 El Niño years during the 81-year period examined here, and these years have been denoted by open circles in Figure 16.7. For 8 out of 18 El Niño events, the normalized rainfall anomaly is less than −1.0, and for 14 out of 18 events the anomaly is negative. However, the predictive value of this relationship is limited only to El Niño years. During the 81-year period examined here, there were 16 instances when the normalized rainfall anomaly was close to or less than −1.0, and 8 out of these 16 cases were not associated with El Niño. If an El Niño event has already been observed in the previous winter and spring, a prediction for drought over India can be made with a high degree of confidence. The relationship between El Niño and monsoon rainfall is applicable for a limited number of cases, namely, the ones when El Niño is observed, whereas the relationship between the Southern Oscillation and monsoon rainfall is applicable in general. Monitoring of both the Southern Oscillation and El Niño can provide very useful guidance for the long-range forecasting of monsoon rainfall over India.

It can be argued that a negative trend in the winter to spring pressure is an indicator of below normal pressure at Darwin during the spring. If so, a combination of Darwin's winter–spring trend and its spring pressure anomaly should provide better guidance for forecasting the anomaly of monsoon rainfall. Figure 16.8 shows a scatter diagram between winter–spring Darwin pressure trend, along the abscissa, and its normalized spring pressure anomaly, along the ordinate. The numbers in the diagram represent the normalized monsoon rainfall anomaly for each of the 81 years. Nine out of 12 years with a normalized rainfall anomaly equal to or greater than 1.0 occur on the left half of the diagram for a negative Darwin pressure trend and 12 out of 14 years with a normalized rainfall anomaly less than −1.0 occur on the right side for positive values of the trend. It is rather remarkable that none of the 17 years with standardized rainfall anomaly less than −1.0 occur in the lower left quadrant of the diagram. In fact, out of 26 years in the lower left quadrant, there are no instances when the magnitude of the normalized rainfall anomaly is greater than 1 standard deviation in the negative sense. Most of the large negative values fall in the upper right quadrant. Out of 13 years with a standardized rainfall anomaly larger than 1.0, only one year (1961) with a value of 2.0, is in the upper right quadrant, and out of 24 years in the upper right quadrant, the rainfall anomaly is greater than or equal to 1.0 only in one year (1961). This scatter diagram suggests that if spring Darwin pressure is lower than its normal value, and if winter to spring trend shows that the Darwin pressure is falling, a prediction of nonoccurrence of drought over India in the subsequent monsoon season would be almost always right; similarly, a positive anomaly in spring Darwin pressure and a positive trend from

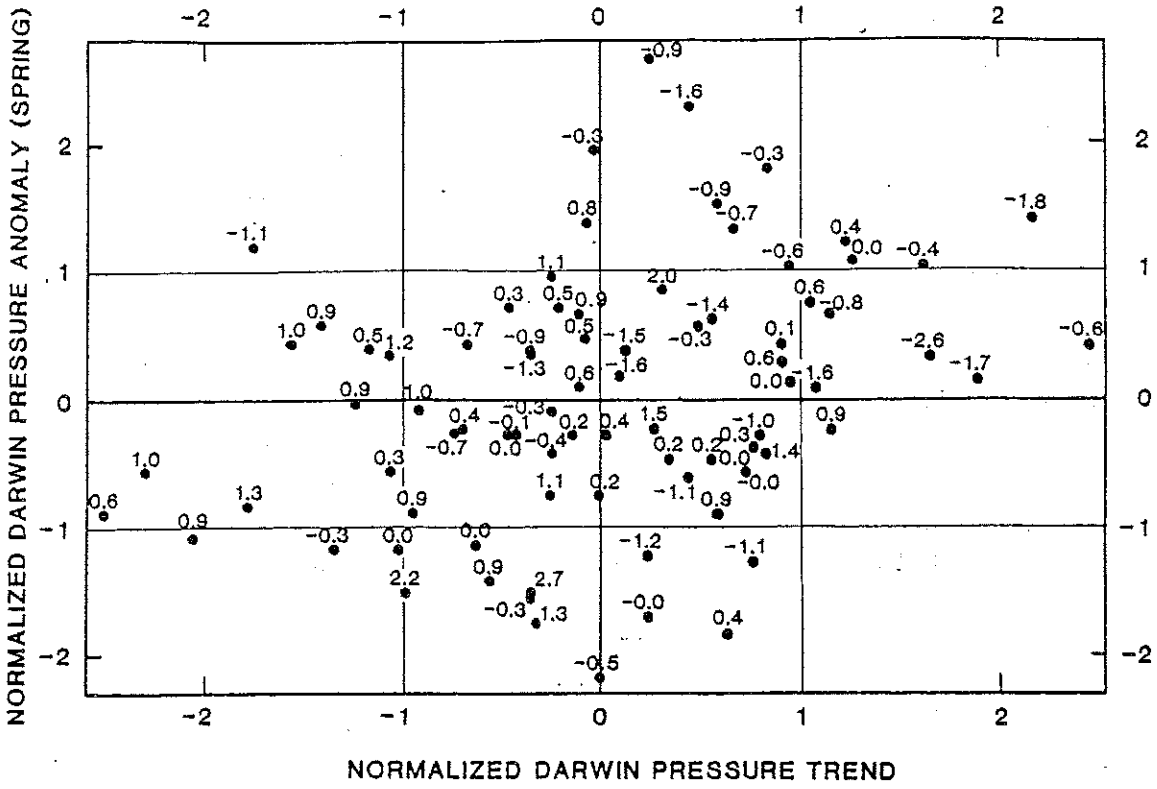

Figure 16.8. Scatter diagram between the normalized Darwin pressure trend (spring–winter) along the abscissa, and normalized spring Darwin pressure anomaly along the ordinate. The numbers denote the normalized Indian monsoon rainfall anomaly. Reprinted with permission from the American Meteorological Society from Shukla and Paolino, *Monthly Weather Review*, **111**, 1830–1837 (1983).

winter to spring would provide a highly reliable forecast of nonoccurrence of excessive monsoon rain.

3.2 Influence of Monsoon Rainfall on the Southern Oscillation

If one is to predict monsoon rain it is necessary to examine the Southern Oscillation before the monsoon season. However, it should be recalled that one of Walker's most important findings was that monsoon rainfall has very significant correlations with the subsequent global circulation. Normand (14) aptly wrote:

> To my mind the most remarkable of Walker's results was his discovery of the control that the Southern Oscillation seemingly exerted upon subsequent events and in particular of the fact that the index for the Southern Oscillation as a whole for the summer quarter June–August, had a correlation coefficient of 0.8 with the same index for the following winter quarter, though only of −0.2 with the previous winter quarter. It is quite in keeping with this that the Indian monsoon rainfall has its connections with later rather than with earlier events. The Indian monsoon therefore stands out as an active, not a passive feature in world weather, more efficient as a broadcasting tool than as an event to be forecast.

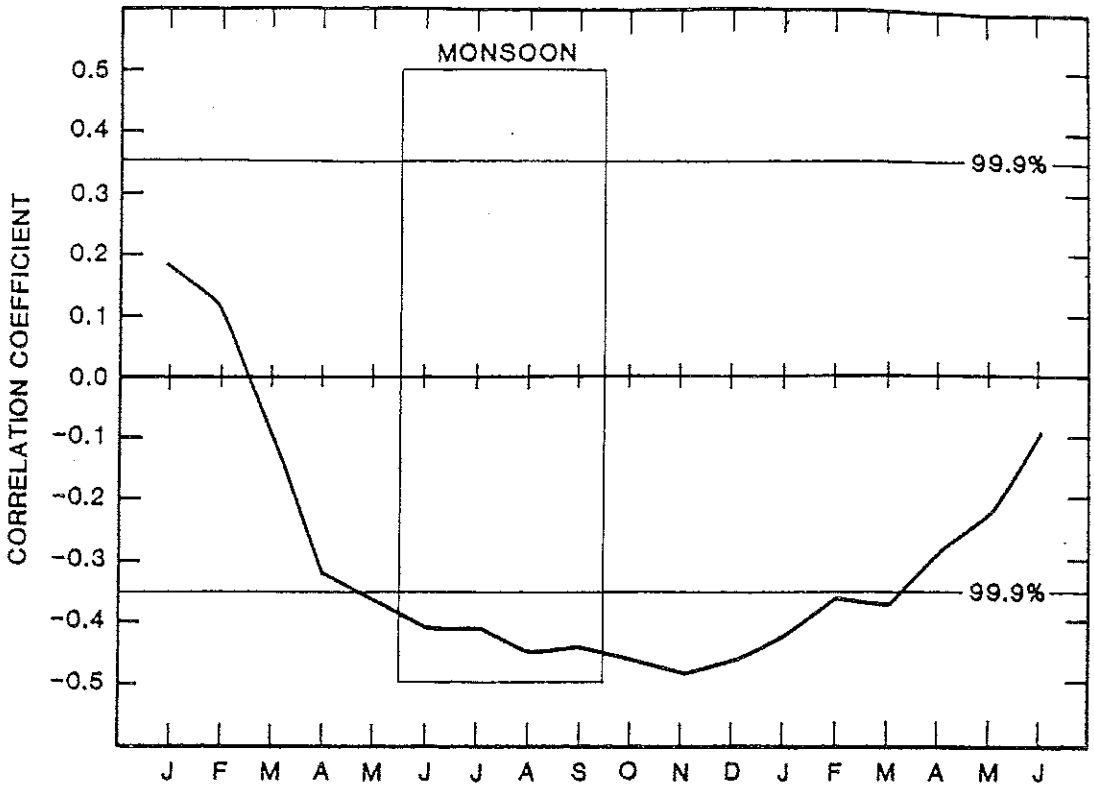

Figure 16.9. Correlation coefficient between the Indian monsoon rainfall anomaly for monsoon season (shown by rectangle) and 3-month mean Darwin pressure anomaly centered at the months shown along abscissa before and after the monsoon season. Reprinted with permission from the American Meteorological Society from Shukla and Paolino, *Monthly Weather Review*, **111**, 1830–1837 (1983).

Figure 16.9 shows the correlation coefficient for 81 years of data of the normalized monsoon rainfall anomaly and the Darwin pressure anomalies from six months before to six months after the monsoon season. The largest negative correlations are found in November following the monsoon season. This suggests a possible role of monsoon rainfall fluctuations (and the associated changes in the location and intensity of heating fields) in affecting the subsequent global circulation. The correlation coefficient between Indian monsoon rainfall anomalies and Darwin minus Tahiti pressure (not shown) is very similar to the one shown in Figure 16.9 with opposite sign.

Figure 16.10 shows the autocorrelation of seasonal mean Darwin pressure anomalies at different seasonal lags. In agreement with the earlier results of Walker, the largest correlation between adjacent seasons is found between summer and fall, and between fall and winter pressure anomalies. The slow decay of autocorrelations from summer to fall and from fall to winter and the largest correlations between monsoon rainfall and Darwin pressure following the monsoon season (Fig. 16.9) suggest a possible role of monsoons in modulating the Southern Oscillation. The smallest correlations between adjacent seasons are found between winter and spring, and spring and summer. This is seen further in Figure 16.11 which shows a scatter diagram between normalized Darwin winter–spring pressure trend and normalized

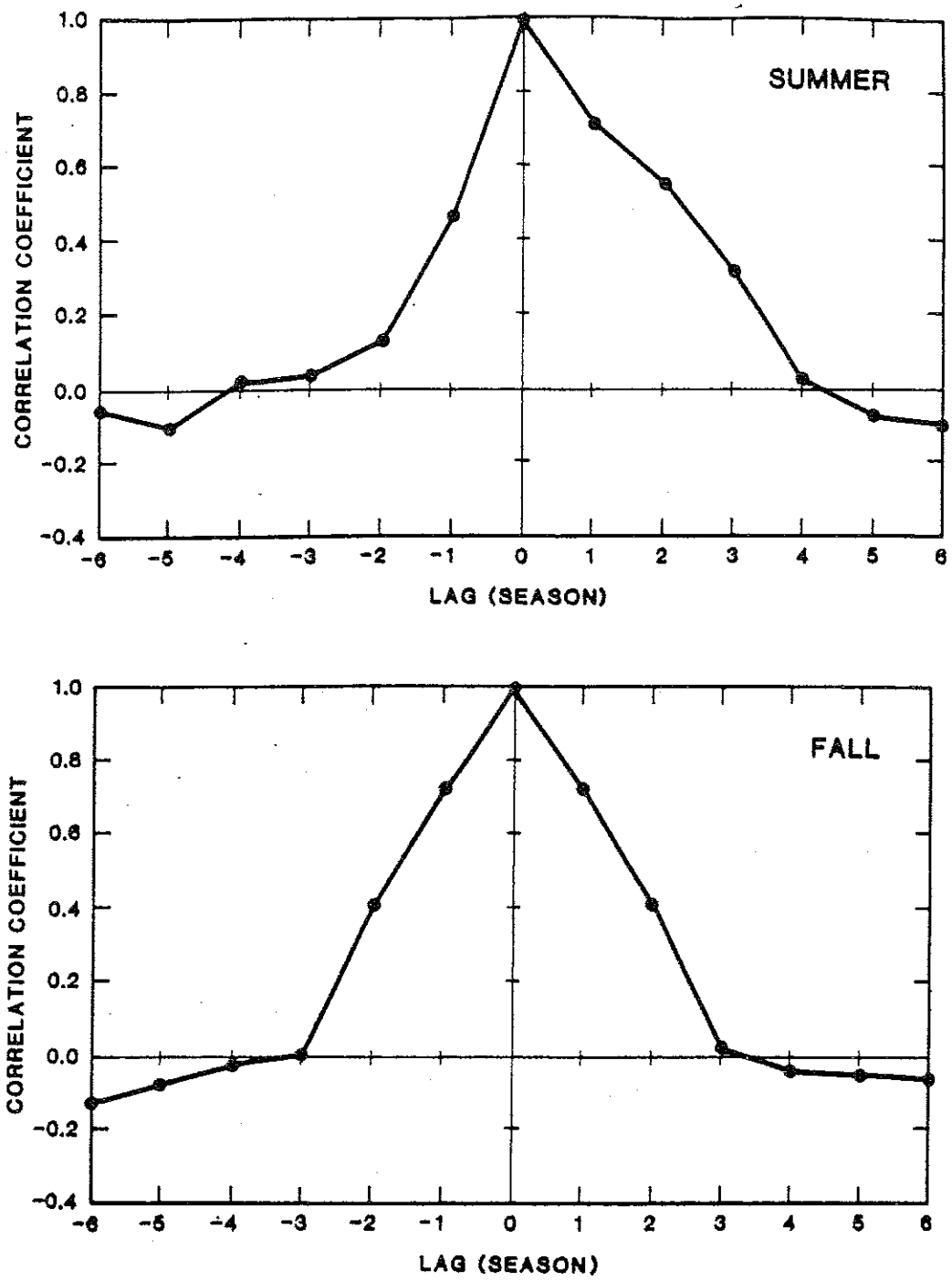

Figure 16.10. Autocorrelation of summer, fall, winter, and spring seasonal mean Darwin pressure anomaly with preceding (negative lags) and succeeding (positive lags) seasons. Reprinted with permission from the American Meteorological Society from Shukla and Paolino, *Monthly Weather Review*, **111**, 1830–1837 (1983). (*Figure 16.10 continues on p. 542.*)

winter Darwin pressure anomaly. The most prominent feature is a strong inverse relationship (correlation coefficient = -0.74) between the winter pressure anomaly and winter to spring trend; if the winter pressure is higher than normal, the (spring–winter) tendency is negative and vice versa. This suggests that Darwin pressure undergoes a marked transition from winter to spring. However, the winter Darwin

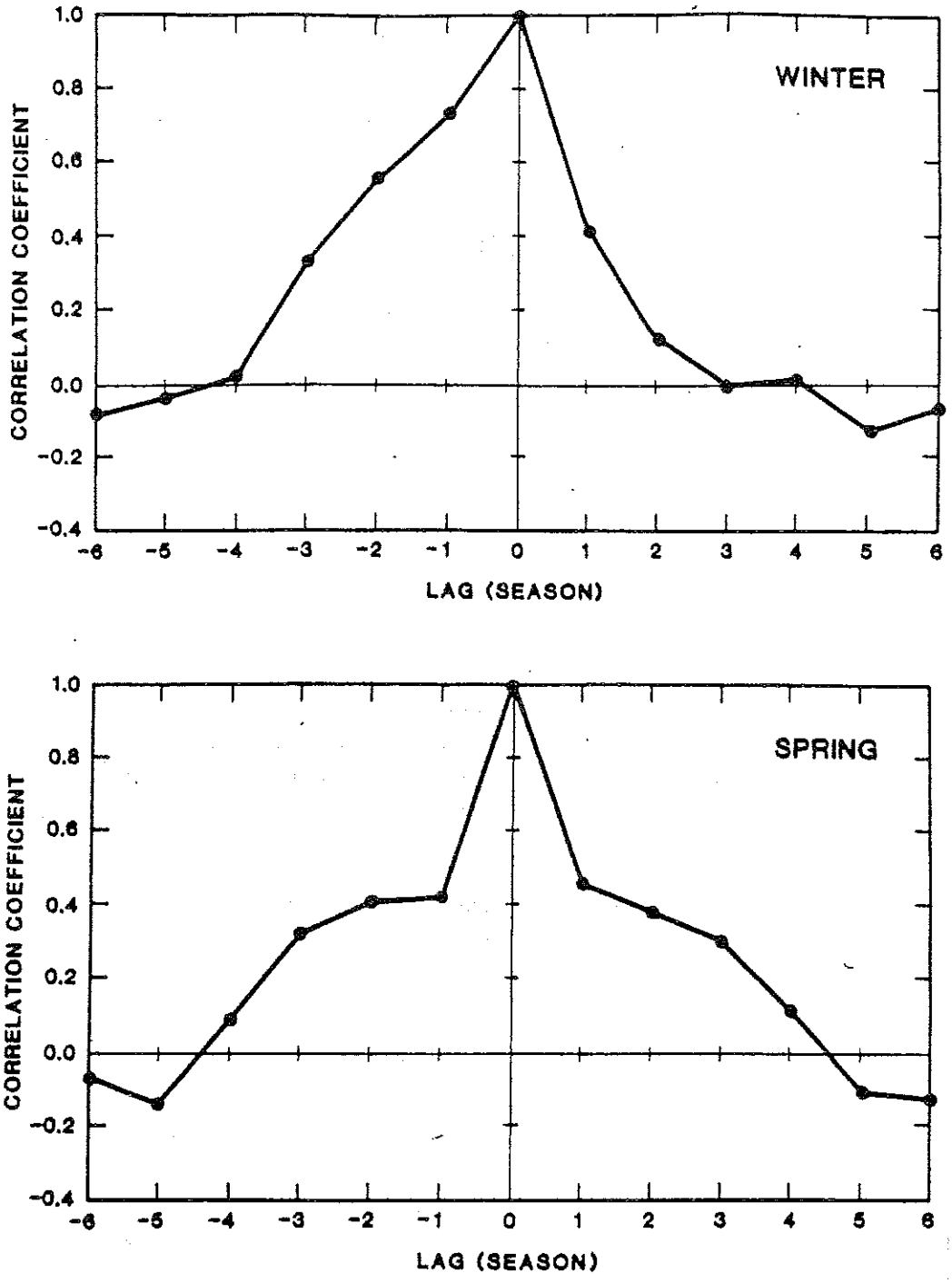

Figure 16.10. (*continued*)

pressure anomaly itself is not found to be of any particular importance for long-range forecasting of monsoon rainfall.

4 SUGGESTIONS FOR FURTHER RESEARCH

Considering the great socioeconomic importance of the fluctuations of monsoon

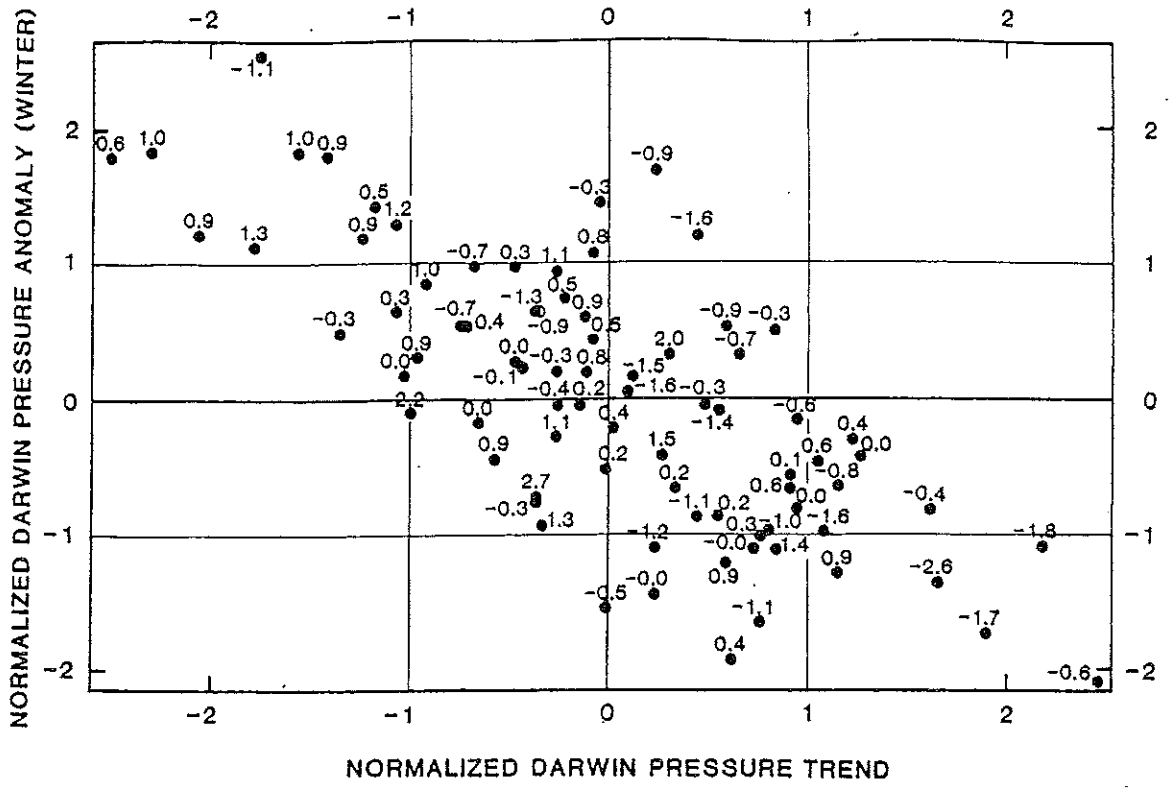

Figure 16.11. Scatter diagram between the normalized Darwin pressure trend (spring–winter) along the abscissa, and normalized winter Darwin pressure anomaly along the ordinate. The numbers denote the normalized Indian monsoon rainfall anomaly. Reprinted with permission from the American Meteorological Society from Shukla and Paolino, *Monthly Weather Review*, **111**, 1830–1837 (1983).

and predictability. Modeling and observational studies should be carried out to determine the influence of global boundary conditions and interrelationships with global circulation features. I believe that global general circulation models are already realistic enough to be used for dynamical prediction of monthly and seasonal anomalies, and that actual forecasts should be carried out with observed global initial and boundary conditions. I also believe that, parallel to this approach, it is also necessary that comprehensive synoptic and statistical studies be carried out to document the nature of monsoon variability and its relation to other tropical and mid-latitude circulation features. We have more data than Walker had 60 years ago, and we also have a better understanding of the mean circulation of the earth's atmosphere. There is reason to believe that a Walker-like effort of massive data analysis and diagnostic studies would provide valuable insights into the nature and causes of monsoon variability. During the recent years we have gained a better understanding of large-scale atmospheric phenomena such as El Niño and the Southern Oscillation, the quasi-biennial oscillation, and atmospheric blocking. This new knowledge provides a better synoptic and dynamical framework to examine the interannual and the long-term variability of monsoons. The El Niño–Southern Oscillation seems to be the single most important feature of the ocean–atmosphere system. Its period is quite large (2–5 years) and therefore it can be of practical value for predicting fluctuations of a seasonal phenomenon like the monsoon. It is

the monsoon, during different phases of the Southern Oscillation. It should, however, be recognized that the fluctuations of the monsoon can also be one of the important factors affecting the Southern Oscillation.

Based on the findings of several recent studies, we recommend a detailed examination of the long-term records for the following circulation features, which are not necessarily independent of each other:

1. sea level pressure over India, Australia, and Southeast Asia;
2. snow cover and snow depth over Eurasia and the Himalayas (21, 22);
3. sea surface temperature over the equatorial Pacific (20);
4. upper air circulation over India, latitudinal position of the 500-mb ridge (23), wind speed and direction over Indian upper air stations (17, 24, 25), upper troposphere thickness anomalies (26), and trough and ridge positions at 50 mb (27);
5. quasi-biennial oscillation (28);
6. blocking in the mid-latitudes (29);
7. convection over Indonesia and the equatorial Pacific;
8. typhoon activity over the western Pacific (30); and
9. boundary conditions and circulation in the Southern Hemisphere.

Combining global circulation parameters, such as those listed above, for different phases of the Southern Oscillation, and for years of droughts and excessive monsoon rainfall, might provide useful insight into the nature of monsoon variability and value of these parameters as potential predictors of monsoon rainfall.

Abilities and limitations of stochastic and dynamic models (31) for long-range forecasting of monsoon rainfall should also be further examined.

5 SUMMARY AND CONCLUDING REMARKS

The prospects for long-range forecasting of large-scale, seasonal mean monsoon rainfall appear to be good. There are significant correlations between large-scale seasonal mean Indian rainfall anomalies and low-frequency changes in the Southern Oscillation. There are also significant correlations between seasonal Indian rainfall anomalies and slowly varying boundary conditions of sea surface temperature and snow cover. Collectively, these observed associations support the notion that the seasonal mean Indian rainfall anomalies are not merely a consequence of random statistical variations in the atmosphere, but are associated with low-frequency, large-scale changes in the global circulation.

Tropical and monsoon flows are dominated by the thermally forced planetary-scale Hadley and Walker type circulations for which the primary energy source is the latent heat of condensation. The large-scale moisture convergence required for the release of the latent energy is organized by gradients of temperature at the

earth's surface. Solar heating can produce thermal low-pressure areas over the land which can further deepen due to latent heating if the dynamical circulation is favorable for moisture convergence. Therefore fluctuations of soil moisture can influence the intensity of the tropical heat sources over the land. Similarly, the tropical heat sources over the oceans can be influenced by the anomalies of sea surface temperature. It is therefore reasonable to expect that the changes in the large-scale tropical flows would be related to the changes in the slowly varying boundary conditions at the earth's surface. Since dynamical instabilities are not too strong in the tropics, it is also reasonable to hypothesize that the changes in the large-scale flows are dominated by the changes in the boundary conditions. These arguments collectively suggest that there is a physical basis for predictability of the large-scale, seasonally averaged monsoon flow and rainfall.

If the daily rainfall patterns related to the monsoon's high frequency, synoptic-scale disturbances were the consequence of dynamical instabilities of the large-scale flow, and if the changes of the large-scale flow itself were caused mainly by its interaction with such unstable disturbances, the prospects for long-range forecasting, beyond the limits of deterministic prediction, would not be very good. Fortunately, this does not appear to be the case. While it is indeed true that the rain producing disturbances form only when the structure of the large-scale flow (i.e., horizontal and vertical gradients of wind, temperature, and moisture) is favorable, the changes in the large-scale flow itself appear to be primarily related to planetary-scale boundary forcing manifested as tropical heat sources and to orographic barriers. This provides a physical basis as well as hope for long-range forecasting of monsoon rainfall. It is also of interest that during the monsoon season, even the biweekly and monthly anomalies have significant spatial coherence, which further suggests that the prospects for predicting biweekly and monthly anomalies are also quite good.

REFERENCES

1. J. Shukla, Dynamical predictability of monthly means, *J. Atmos. Sci.*, **38**, 2547–2572 (1981).
2. J. Shukla, "Predictability of Time Averages: Part II. The Influence of the Boundary Forcing," in D. M. Burridge and E. Kallen, Eds., *Problems and Prospects in Long and Medium Range Weather Forecasting*, Springler-Verlag, London, 1984, pp. 155–206.
3. J. G. Charney and J. Shukla, "Predictability of Monsoons," in Sir James Lighthill, and R. P. Pearce, Eds., *Monsoon Dynamics*, Cambridge University Press, Cambridge, 1981, pp. 99–110.
4. J. G. Charney, W. J. Quirk, S. Chow, and J. Kornfield, A comparative study of the effects of albedo change on drought in semi-arid regions, *J. Atmos. Sci.*, **34**, 1366–1385 (1977).
5. S. Manabe and D. G. Hahn, Simulation of atmospheric variability, *Mon. Wea. Rev.*, **109**, 2260–2286 (1981).
6. J. Shukla, "Predictability of the Tropical Atmosphere," NASA Tech. Memo. 83829, NASA/Goddard Space Flight Center, Greenbelt, MD, 1981.

7. N.-C. Lau, A diagnostic study of recurrent meteorological anomalies appearing in a 15-year simulation with a GFDL general circulation model, *Mon. Wea. Rev.*, **109**, 2287–2311 (1981).
8. R. A. Madden, Estimates of the natural variability of time-averaged sea level pressure, *Mon. Wea. Rev.*, **104**, 942–952 (1976).
9. J. Shukla and D. S. Gutzler, Interannual variability and predictability of 500 mb geopotential heights over the Northern Hemisphere, *Mon. Wea. Rev.*, **111**, 1273–1279 (1983).
10. B. J. Hoskins and D. Karoly, The steady linear response of a spherical atmosphere to thermal and orographic forcing, *J. Atmos. Sci.*, **38**, 1179–1196 (1981).
11. H. F. Blanford, On the connexion of the Himalaya snowfall with dry winds and seasons of droughts in India, *Proc. Roy. Soc. London*, **37**, 3 (1884).
12. H. H. Hildebrandsson, Quelques recherches sur les entres d'Action de l'Atmosphere, *Kon. Svenska Vetens.-Akad. Handl.*, **29**, 33 (1897).
13. N. Lockyer and W. J. S. Lockyer, On the similarity of the short-period pressure variation over large areas, *Proc. Roy. Soc. London*, **73**, 457–470 (1902).
14. C. Normand, Monsoon seasonal forecasting, *Quart. J. Roy. Meteor. Soc.*, **79**, 463–473 (1953).
15. G. T. Walker, Correlations in seasonal variations of weather, X, *Mem. India. Meteor. Dept.*, **24**, 333–345 (1924).
16. P. Jagannathan, "Seasonal Forecasting in India, A Review," Special Publication No. DGO.82/650, India Meteorology Department, New Delhi, 1960.
17. P. Jagannathan and M. L. Khandekar, Predisposition of upper air structure in March to May over India to the subsequent monsoon rainfall of the peninsula, *Indian J. Meteor. Geophys.*, **13**, 305–316 (1962).
18. G. B. Pant and B. Parthasarathy, Some aspects of an association between the Southern Oscillation and Indian summer monsoon, *Arch. Meteor. Geoph. Biokl., Ser. B.*, **29**, 245–252 (1981).
19. P. B. Wright, "An Index of the Southern Oscillation," Climatic Research Unit Report No. CRU RP4, University of East Anglia, Norwich, U.K., 1975.
20. E. M. Rasmusson and T. H. Carpenter, The relationship between eastern equatorial Pacific sea surface temperature and rainfall over India and Sri Lanka, *Mon. Wea. Rev.*, **111**, 517–528 (1983).
21. D. Hahn and J. Shukla, An apparent relationship between Eurasian snow cover and Indian monsoon rainfall, *J. Atmos. Sci.*, **33**, 2461–2463 (1976).
22. R. R. Dickson, Eurasian snow cover vs. Indian monsoon rainfall—An extension of the Hahn-Shukla results, *J. Clim. and Appl. Meteor.*, **23**, 171–173 (1984).
23. A. K. Bannerjee, P. N. Sen, and C. R. V. Raman, On foreshadowing southwest monsoon rainfall over India with mid-tropospheric circulation anomaly of April, *Indian J. Meteor. Hydrol. Geophys.*, **29**, 425–431 (1978).
24. P. V. Joseph, Sub-tropical westerlies in relation to large scale failure of Indian monsoon, *Indian J. Meteor. Hydrol. Geophys.*, **29**, 412–418 (1978).
25. P. V. Joseph, R. K. Mukhopadhyaya, W. V. Dixit, and D. V. Vaidya, Meridional wind index for long range forecasting of Indian summer monsoon rainfall, *Mausam*, **32**, 31–34 (1981).
26. R. K. Verma, Importance of upper tropospheric thermal anomalies for long range forecasting of Indian summer monsoon, *Mon. Wea. Rev.*, **108**, 1072–1075 (1980).
27. V. Thapliyal, "Stratospheric Circulations in Relation to Summer Monsoon over India," Proc. of Hydrological Aspects of Droughts I. India Meteorology Department, New

28. K. S. Rao Raja and N. J. Lakhole, Quasi-biennial oscillation and summer southwest monsoon, *Indian J. Meteor. Hydrol. Geophys.*, **29**, 403–411 (1978).
29. M. Tanaka, Interannual fluctuations of the tropical easterly jet and the summer monsoon in the Asian region, *J. Meteor. Soc. Japan*, **60**, 865–875 (1982).
30. M. Kanamitsu and T. N. Krishnamurti, Northern summer tropical circulations during drought and normal rainfall months, *Mon. Wea. Rev.*, **106**, 331–347 (1978).
31. V. Thapliyal, Stochastic dynamic model for long range prediction of monsoon rainfall in peninsular India, *Mausam*, **33**, 399–404 (1982).